OFF-ROAD SOFT SOIL TIRE MODEL DEVELOPMENT AND EXPERIMENTAL TESTING

Dr. Corina Sandu[1], Mr. Eduardo Pinto[2], Mr. Scott Naranjo[3], Dr. Paramsothy Jayakumar[4], Dr. Archie Andonian[5], Dr. Dave Hubbell[6], Dr. Brant Ross[7]

[1]Virginia Tech, [2]Virginia Tech, [3]Virginia Tech, [4]TARDEC, [5]The Goodyear Tire & Rubber Company, [6]The Goodyear Tire & Rubber Company, [7]MotionPort
csandu@vt.edu

Abstract

The goal of this paper is to present an accurate, comprehensive, and efficient, off-road tire model for soft soil applications (traction, handling, ride, and vehicle durability) as needed to support current Army simulation needs. The literature review revealed that, while FEM lead to the most detailed tire-soil models, their complexity and extensive computational effort make them less than ideal for the applications envisioned. The proposed approach is a detailed semi-analytical tire model for soft soil that utilizes tire construction details which parallel commercially available on-road tire models. The novelty relies on increasing the level of details for the tire model, in improving the tire-soil interface model by enhancing the resolution of the tire model at the contact patch, and by accounting for effects and phenomena not considered in existing models. The model will be validated against experimental data. For low speed, testing will be done on a single tire on sandy loam in the terramechanics rig at Virginia Tech. The influence of tire and vehicle parameters on the contact patch forces and on the forces transmitted to the axle will be investigated. The effect of soil characteristics on the tire dynamics will be studied. Validation against data collected from full vehicle testing is included in the proposed future work.

Keywords: tire model, soft soil, terramechanics, vehicle dynamics, indoor testing

1 Introduction

The goal of this paper is to present an accurate, comprehensive, and efficient, off-road tire model for soft soil applications (traction, handling, ride, and vehicle durability) as needed to support current Army mobility goals. The literature review revealed that, while finite element method (FEM) leads to the most detailed tire-soil models, their complexity and extensive computational effort make them less than ideal for the applications envisioned. The proposed approach is a detailed semi-analytical tire model for soft soil that utilizes tire construction details which parallel commercially available on-road tire models. The novelty relies on increasing the level of details for the tire model, in improving the tire-soil interface model by enhancing the resolution of the tire model at the contact patch and by accounting for effects and phenomena not considered in existing models. The model will be validated against experimental data. For low speed, testing is conducted on a single tire on sandy loam in the terramechanics rig at Virginia Tech. The influence of tire and vehicle parameters on the contact patch forces and on the forces transmitted to the axle will be investigated. The effect of soil characteristics on the tire dynamics will be studied.

2 Literature Review

Most tire models are developed with a particular application in mind. Depending on

Report Documentation Page

Form Approved
OMB No. 0704-0188

1. REPORT DATE	2. REPORT TYPE	3. DATES COVERED
29 JUN 2011	**Journal Article**	**09-11-2010 to 12-05-2011**

4. TITLE AND SUBTITLE
OFF-ROAD SOFT SOIL TIRE MODEL DEVELOPMENT AND EXPERIMENTAL TESTING

5a. CONTRACT NUMBER
5b. GRANT NUMBER
5c. PROGRAM ELEMENT NUMBER

6. AUTHOR(S)
Corina Sandu; Eduardo Pinto; Scott Naranjo; Paramsothy Jayakumar; Archie Andonian

5d. PROJECT NUMBER
5e. TASK NUMBER
5f. WORK UNIT NUMBER

7. PERFORMING ORGANIZATION NAME(S) AND ADDRESS(ES)
Virginia Tech,965 Prices Fork Road,Blacksburg,VT,24061

8. PERFORMING ORGANIZATION REPORT NUMBER
; #21973

9. SPONSORING/MONITORING AGENCY NAME(S) AND ADDRESS(ES)
U.S. Army TARDEC, 6501 East Eleven Mile Rd, Warren, Mi, 48397-5000

10. SPONSOR/MONITOR'S ACRONYM(S)
TARDEC

11. SPONSOR/MONITOR'S REPORT NUMBER(S)
#21973

12. DISTRIBUTION/AVAILABILITY STATEMENT
Approved for public release; distribution unlimited

13. SUPPLEMENTARY NOTES
For 17TH INTERNATIONAL CONFERENCE OF THE INTERNATIONAL SOCIETY FOR TERRAIN-VEHICLE SYSTEMS-SPETEMBER 18-22, 2011, BLACKSBURG, VIRGINIA

14. ABSTRACT
The goal of this paper is to present an accurate, comprehensive, and efficient, off-road tire model for soft soil applications (traction, handling, ride, and vehicle durability) as needed to support cur-rent Army simulation needs. The literature review revealed that, while FEM lead to the most de-tailed tire-soil models, their complexity and extensive computational effort make them less than ideal for the applications envisioned. The proposed approach is a detailed semi-analytical tire model for soft soil that utilizes tire construction details which parallel commercially available on-road tire models. The novelty relies on increasing the level of details for the tire model, in improving the tire-soil interface model by enhancing the resolution of the tire model at the contact patch, and by ac-counting for effects and phenomena not considered in existing models. The model will be validated against experimental data. For low speed, testing will be done on a single tire on sandy loam in the terramechanics rig at Virginia Tech. The influence of tire and vehicle parameters on the contact patch forces and on the forces transmitted to the axle will be investigated. The effect of soil charac-teristics on the tire dynamics will be studied. Validation against data collected from full vehicle testing is included in the proposed future work.

15. SUBJECT TERMS
tire model, soft soil, terramechanics, vehicle dynamics, indoor testing

16. SECURITY CLASSIFICATION OF:			17. LIMITATION OF ABSTRACT	18. NUMBER OF PAGES	19a. NAME OF RESPONSIBLE PERSON
a. REPORT	b. ABSTRACT	c. THIS PAGE			
unclassified	**unclassified**	**unclassified**	**Public Release**	**14**	

Standard Form 298 (Rev. 8-98)
Prescribed by ANSI Std Z39-18

the application, a compromise needs to be made between computational efficiency, accuracy, resolution, and ease of parametrization. Fig. 1 illustrates the classification of tire models based on the approach used, in increasing order of complexity, and their applications. At the bottom of the diagram are the least complex models such as the empirical Pacejka-type models; at the very top are the very complex finite element models.

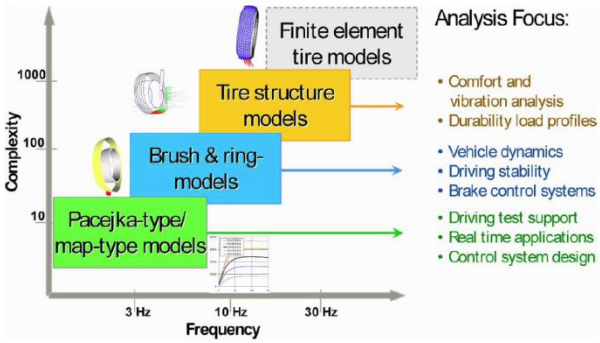

Fig. 1: *Tire model types and their intended applications [1]*

A brief overview of the tire models in each of these classes is presented next.

2.1 Empirical Tire Modelling

Empirical tire models rely on modelling the tire performance by curve-fitting a very large amount of experimental data. Most of the time the mathematical formulations thus obtained do not carry a physical significance, and are specific for each tire simulated. The most important areas of application for empirical models are mobility and real-time simulations. Perhaps the most important empirical tire model is the Waterways Experimental Station (WES) mobility model [2]. This is a "*go/no go*" model that uses an instrument called a cone penetrometer to determine a cone index, which is then compared to a mobility index of a vehicle. The vehicle mobility index is computed based on vehicle characteristics such as vehicle weight, contact area, size of grouser, engine power, and type of transmission. If the vehicle mobility index exceeds the cone index then motion is possible; otherwise the vehicle is stuck.

Wismur-Luth [3-4] also developed an empirical model using bias-ply tires. When radial tires are used, the Wismur-Luth model tends to under-predict the traction of the vehicle. Most models that originated from the Wismur-Luth model used variations of the Wismur-Luth equations to account for changes in experimental conditions, including the use of radial-ply tires. Brixius [5] developed a traction prediction model for bias-ply tires based on similar methods, and suggested modifications of the relations for radial tires. However, Upadhyaya and Wulfsohn stressed in [6] that the empirical traction models seldom provided any insight into the underlying mechanics and should be used with caution when evaluating new tire situations.

2.2 Semi-analytical Tire Modelling

Semi-analytical tire models are probably the most versatile models because they provide good fidelity, while also having physical significance. Their large spectrum of complexity makes them suitable for a large variety of applications. The simplest semi-analytical models are the single point contact models, mostly used for ride applications. There are also complex semi-analytical tire models used for a variety of vehicle dynamics simulations. Most semi-analytical tire models simulations run close to real time.

The FTire [7] is arguably the most widely used commercial semi-analytical tire model for on-road applications. This model discretizes the tire in *N* discrete masses (in a single plane) to model the tire. By using torsional springs and shape functions the model predicts the tire behaviour in the lateral direction. A simple contact model based on Bekker's equations is available for off-road simulations. Other tire models based on a similar semi-analytical approach are the CD-Tire 40 [8] and RMOD-K [9].

Chan [10] has previously developed flexible ring and rigid tire models that are used for on-road and off-road vehicle dynamics and vehicle mobility applications. Lee et al. [11] developed a semi-analytical model for snow where the snow is modelled as a depth-dependant modified Drucker-Prager material.

This model, as well as Chan's model, use a combined slip formulation. El-Gawwad et al. [12-13] developed a multi-spoke tire model using Bekker's pressure-sinkage formula and included the effect of straight lugs on vehicle-terrain interaction for an agricultural tire. This tire model accounts for parameters which affect vehicle maneuvering, such as slip angle, soil deformation modulus, lug dimensions, and lug spacing. Harnisch developed a model for both rigid and elastic tires, where the elastic tire model "*uses a larger substitute circle to describe the deformed contact patch between the tyre and soil*" [14]. The substitute circle diameter is obtained from the equilibrium between the vertical reaction force of the soil and the normal force applied to the tire.

2.3 Finite Element Tire Modelling

The use of the finite element methods to model tires flourished in the last two decades, mostly because of the increase in computing power available. Fervers [11] created a model that uses a multi-layered ring to model the different components in the tire. Given the complexity and time required to create and run a three dimensional model he transfers 3D elements into a 2D half-space to save on computing time. The results from this study are encouraging in the sense that it demonstrates that a detailed model that includes the different layers of the tire adds to the resolution of the model; proving that a detailed model can capture with a good resolution the tire dynamics of off-road simulations.

Nakashima and Oido [12] discussed a method to combine Finite Element Analysis (FEA) and Discrete Element Analysis (DEA) to model tire-soil behavior. The soil is modeled using DE while the tire is modeled using FE. The main purpose of this study is to better describe the microscopic deformation of the soil. Lee et al. [30] also employs an FE model for fresh, low-density snow. In this study the snow is simulated as a pressure-sensitive Drucker-Prager material in order to establish the relationship between strengths in compression/tension.

One of the most representative FE tire models is Shoop's model [15]. For simulations, a Drucker-Prager snow model is used. Composite material properties are used to model the different parts of the tire. The model predicts the forces at the wheel axle, but it is still computationally expensive.

2.4 Literature Review for Tire Testing

Throughout the years of studies in vehicle performance, particularly on deformable soils, a variety of instrumented vehicles, trailers, and indoor single-tire testing platforms have been constructed to aid in understanding the tire-soil interaction. Using such test facilities and equipment it was possible to gather relevant test results. It is important to be familiar with these past studies in order to design future experiments. Since the Advanced Vehicle Dynamics Lab at Virginia Tech has a single wheel testing unit, most of the testing methods reviewed here will revolve around that of a single wheel test.

The overall focus of building a controlled tire testing device is to investigate tire performance, such as traction, under known normal loads and controlled slip conditions. The information collected supports tire models validation and helps understand the tire performance under given conditions. It may also help in controlling soil compaction, improving the protection of the environment, increasing soldier safety, and optimizing the tire design for performance and energy efficiency.

Among all the different types of tire testing platforms, indoor soil bins appear to be an appropriate experimental method to follow, especially for terramechanics, due to the capability of controlling the soil conditions. This proved necessary in early field tractor tire testers which would suffer from soil discontinuities [16]. A single wheel test device consists of a carriage that can move at its own speed simulating a vehicle, via a motor-chain system, and houses the test wheel and any sort of instrumentation of interest. The carriage can also house the motor that drives the wheel independently; this allows the possibility of

testing any desired longitudinal slip. The carriage, which acts like a quarter-car model without a suspension system, can run a test tire over the conditioned soil in the soil bin.

The indoor soil bins allow the investigator to mix and compact the soil as desired, run a test, then repeat the reconditioning process. However, constantly reconditioning the soil after every test run and having limited space can make this method tedious and constricting. The mix and compaction procedure would begin by tilling the soil, leveling it, and then applying a load to compact the soil to a desired uniform density. Rather than manually reconditioning the soil with rakes and rollers, some studies have developed automated devices that process the soil as needed before each test run as done in the study at Kyoto University in Japan [17]. In this agricultural study, a device was fitted in the single wheel test rig to till, level, and compact the water-filtration type sand. This "Mixing-and-Compaction" had a tiller in the front and an aluminum plate in the rear which would flatten the sand surface [17]. To operate the device, a motor-driven roller was attached in the rear, and it was also used to compact the soil.

The type of tire test would also dictate how the soil should be reconditioned, as discussed in the study from the Department of Biological and Agricultural Engineering in University Putra Malaysia, UPM [18]. In this study, two different soil reconditioning methods were used with either a driven-wheel or a towed-wheel. Both compaction procedures began by loosening up the sand to at least 150 mm depth with a hand hoe, then leveling it by hand [19]. If in driven-wheel mode, steel-tubed rollers filled with concrete were hand rolled across the soil bin [18]. If in towed-wheel mode, a heavy gasoline-powered soil compactor was run across the soil surface equipped with a vibrating plate.

Aside from reconditioning the soil after every test run, some tests have been performed to disregard that step in order to explore multi-pass effects [20]. The goal of this sort of test is to simulate the rear wheel of a vehicle rolling along the same path, or rut, left by the front wheel.

Performing tests such as a multi-pass tests, involves several factors; one key factor that the investigator can control is the longitudinal speed of the wheel carriage. The longitudinal slip typically ranges from 0-100%, but can also go to -100% [2]. When performing constant-slip tests, the carriage and test wheel go at their respective velocities at a constant rate, as defined by the investigator at the start of a test, for the effective rolling radius. Although the drawbar pull, F_d, defined as the difference between the tractive effort and the resultant resistance force, can be controlled as well in certain single wheel devices, it was concluded from a Waterways Experiment Station (WES) study that controlled-slip tests are better than controlled-pull tests for defining pull-slip and torque-slip relations [16,2]. It is also interesting to note that in this WES study, wheel performance, as described by controlled-slip tests, was found to be independent of the starting conditions once the selected slip is attained [16]. This conclusion has been reinforced by the recent study conducted by Woodward at NASA GRC [21].

From all the studies reviewed, including some that are not discussed here due to space restrictions, it is well understood that using a systematic methodology, with known influencing factors, it is possible to correlate single wheel testing results to those obtained from full-vehicle testing [16].

3 Model Overview

The proposed soft soil tire model is intended for mobility, traction, ride, handling, and durability applications, for which a complex semi-analytical tire modelling approach is the best fit, when also taking into account its computational efficiency. The schematic of the proposed model can be observed in Fig. 2. It is a discretized lumped mass approach that uses springs and dampers in multiple configurations to represent the different sections of the tire. The model is structured in three parallel planes, two of them representing the side-

walls, and one of them represents the belt and the tread of the tire. By differentiating between the sidewall and the belt a more realistic application of the local forces can be implemented. Each plane consists of N_m number of masses; N_m is suggested between 80 and 100, but it is user defined. This approach has the advantage of being modular and it allows the user flexibility in determining the resolution of the model.

Each lumped mass has three degrees of motion: the translational motion in all directions. Moreover, there is relative motion between masses in the same plane and between masses in adjacent planes, as well. Relative motion is also allowed between lumped masses and the rigid wheel in the circumferential direction, which is a novelty introduced by this model. The wheel has all six degrees of freedom. The total degrees of freedom of the model are,

$$DOF = 9N_m + 6 \tag{1}$$

The shape of the contact patch is assumed to be a curved trapezoid to accommodate transient situations such as sudden steering maneuvers; during quasi-steady-state situations the shape will switch to a curved rectangle, which according to the literature [19-21] is a good assumption for such conditions.

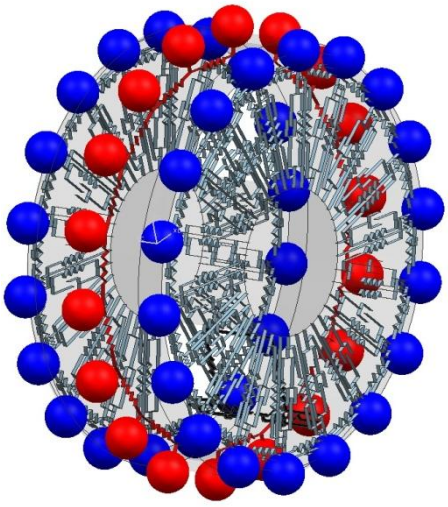

Fig. 2: *3-Dimensional view of the tire model*

3.1 Sidewall Element

The sidewall element is more complex than the belt and tread element because it is directly connected to the rigid wheel. A diagram of the model can be observed in Fig. 3. The mass of a single sidewall element is calculated using Eq.(2).

$$m_{i,s} = \frac{0.5m_{sidewall}}{N_m} \tag{2}$$

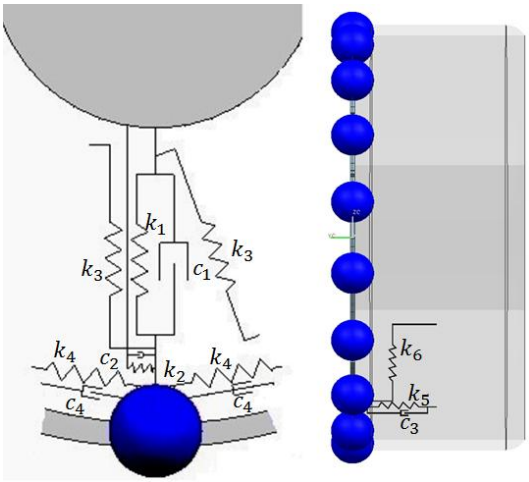

Fig. 3: *Sidewall diagram. Left- the in-plane connections; right - the out-of-plane connections*

3.2 Belt and Tread Element

The belt and tread element is similar to the sidewall element, except it lacks the connection to the rigid wheel. The diagram for the belt and tread element can be found in Fig. 4.

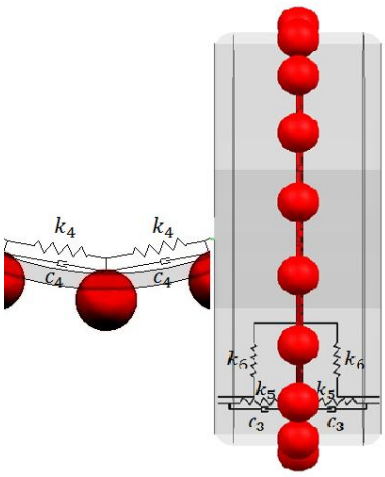

Fig. 4: *Belt and tread element diagram. Left - the in-plane connections; right - the out-of-plane connections.*

It is also important to note that the belt and tread plane has a larger radius, thus, accounting for the curved shape of the tire.

The mass of a single belt and tread element is calculated using the equation,

$$m_{i,bt} = \frac{m_{tread} + m_{belt}}{N_m} \tag{3}$$

4 Tire – soft soil interaction

4.1 Pressure-sinkage relationship

One of the most important aspects of the interaction of the tire with soft soil is the computation of the tire sinkage. In this study we implement an approach developed by Grahn [23], which is a method derived from Bekker's formulation [2], but with additional features; it includes the effects of longitudinal slip, vehicle velocity, and vertical penetration velocity. The results by Grahn shown in Fig. 5 demonstrate the large influence that penetration velocity has on the pressure-sinkage relationship, thus motivating the need to account for it in our model.

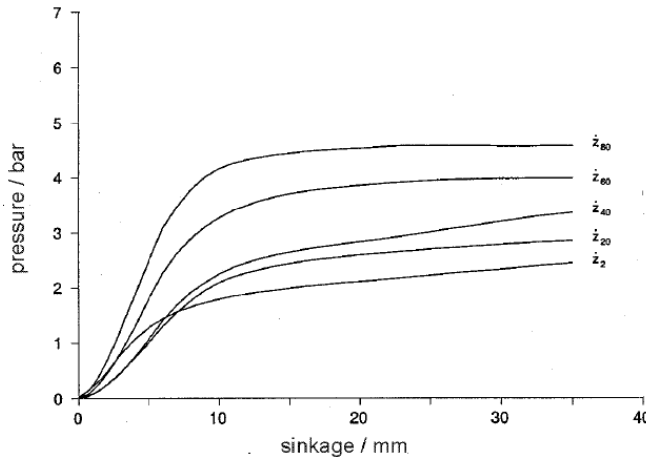

Fig. 5: *Pressure-sinkage relationships for different vertical penetration velocities [2]*

Using this methodology, the sinkage is computed for each mass in the discretized tire model. The pressure in the radial direction on each mass can be computed using Eq. (4)-(5) Note that if $m = 0$ then these equations yield Bekker's quasi-static formulation. All the variables are defined in the nomenclature table.

$$p(\theta) = k_0 z(\theta)^n \dot{z}(\theta)^m \tag{4}$$

$$p(\theta) = k_0 z(\theta)^n \left[\frac{V_x}{1 - s_d} \sin\left[\arccos\left(1 - \frac{z_0 - z(\theta)}{R_l(\theta)}\right)\right]\right]^m \tag{5}$$

4.2 Shear Stress

The shear stress in the contact patch is computed using Janosi and Hanamoto's approach [2]. In this approach the longitudinal shear displacement is calculated at each mass by integrating the tangential slip velocity over time yielding the following equation,

$$j_x(\theta) = R_l(\theta)[(\theta_e - \theta) - (1 - s_d)(\sin\theta_e - \sin\theta)] \tag{6}$$

On the other hand, the lateral shear displacement is calculated by integrating the lateral velocity over time, thus, the equation below,

$$j_y(\theta) = R_l(\theta)(1 - s_d)(\theta_e - \theta)\tan\alpha_c \tag{7}$$

Once the shear displacements are calculated, the shear stress can be evaluated using Bekker's approach [24] at each mass ,

$$\tau(\theta) = \tau_{max}\left(1 - e^{-\frac{j(\theta)}{k}}\right) \tag{8}$$

Nonetheless, in order to account for a combined slip scenario, the shear strength envelope of the soil needs to be defined. This is done by implementing the Mohr-Coulomb failure criteria, where the inequality in Eq. (9) bounds the shear stress.

$$\left(\frac{\tau_x}{\tau_{max}}\right)^2 + \left(\frac{\tau_{ycp}}{\tau_{max}}\right)^2 \leq 1 \tag{9}$$

$$\tau_{max} = (c + \sigma_n(\theta)\tan(\phi)) \tag{10}$$

Substituting Eq. (10) into Eq. (9) and θ_a for θ in both Eqs. (6) and (7) yields the following:

$$\left(1 - e^{\frac{-R_l[(\theta_e-\theta_a)-(1-s_d)(\sin\theta_e-\sin\theta_a)]}{k_x}}\right)^2 + \left(1 - e^{\frac{-(R_l(1-s_d)(\theta_e-\theta_a)\tan\alpha_c)}{k_y}}\right)^2 = 1 \quad (11)$$

where θ_a is the angle of transition between adhesion and sliding. Thus, by solving numerically for θ_a in Eq. (11) the shear stress can be obtained using Eqs. (11), (12) and (13).

$$\tau_x = \begin{cases} \tau_{max}\left(1 - e^{\frac{-R_l[(\theta_e-\theta_a)-(1-s_d)(\sin\theta_e-\sin\theta_a)]}{k_x}}\right) & \theta_e > \theta \geq \theta_a \\ \tau_{max} & \theta_a > \theta \geq -\theta_r \end{cases} \quad (12)$$

$$\tau_{ycp} = \begin{cases} \tau_{max}\left(1 - e^{\frac{-(R_l(1-s_d)(\theta_e-\theta_a)\tan\alpha_c)}{k_y}}\right) & \theta_e > \theta \geq \theta_a \\ \tau_{max} & \theta_a > \theta \geq -\theta_r \end{cases} \quad (13)$$

4.3 Normal Stress

For rigid driven wheels the location of maximum normal stress is located below the wheel axle, which is the lowest part of the tire. Experimental results show that the location of maximum pressure for a pneumatic tire is somewhere between the entry and exit angles and its location is dependent on slip ratio [24]. Thus, in order to account for this phenomena, Wong's approach [24] is to determine the sinkage of each mass by first determining the angle of maximum normal stress θ_m. The experimental constants c_0 and c_m are both a function of normal load and inflation pressure.

$$\theta_m = [c_0(F_z, p_t) + c_m(F_z, p_t)|s_d|]\theta_e \quad (14)$$

Based on this angle of maximum normal stress the sinkage is defined in two sections. The sinkage from the entry angle to the maximum stress angle is determined from the following formulation,

$$z(\theta) = R_l(\theta)(\cos\theta - \cos\theta_e) \quad (15)$$

The sinkage from the maximum stress angle to the exit angle is calculated using Eq. (16),

$$z(\theta) = R_l(\theta)\left(\cos\left(\theta_e - \left(\frac{\theta - \theta_r}{\theta_m - \theta_r}\right)(\theta_e - \theta_m)\right) - \cos\theta_e\right) \quad (16)$$

The maximum sinkage is evaluated by Eq. (17).

$$z_0 = R_l(\theta_m)(\cos\theta_m - \cos\theta_e) \quad (17)$$

For straight line driving at zero camber, a parabolic distribution of the pressure in the contact patch in the longitudinal direction is an accurate representation. The shape of the contact patch in this case is close to rectangular. Most existing tire models assume a uniform distribution of the pressure in the lateral direction of the contact patch. In this study, a parabolic distribution will be considered in the lateral direction during steady-state maneuvers. However, for cornering maneuvers and driving with a non-zero camber angle, a trapezoid is a more accurate representation of the contact patch; in this case, the pressure distribution in the lateral direction is no longer symmetric, as it is assumed for straight line driving at zero camber.

The first step in the simulation is to load the tire. Thus, by substituting Eqs. (14)-(17) into Eq. (5) and using a quasi-steady state equilibrium for the tread and belt masses in the radial direction, the following equation is obtained:

$$m_i\ddot{z}_i + k_6\left(2R_{l,i} - R_{l,i,sidewall,left} - R_{l,i,sidewall,right}\right) = -W_i\sin\theta_i + \sigma_{n,i} + \tau_{x,i}\sin\theta_i \quad (18)$$

Where the radial direction is, in fact, the normal direction in which the pressure is applied on each mass element.

$$\sigma_n(\theta) = p(\theta) \quad (19)$$

By replacing Eq. (19) into (18) an equation with both R_l and θ_e is obtained. Thus, additional information is needed, in order to approximate the initial loaded radius of the tire. The formulation used to approximate the initial loaded radius of each mass is based on the approach developed by Sandu and Chan in [16]. The main difference is that in the current study the sidewalls and the tread and belt elements will have different effective rolling radii, since they are located in different planes. Based on this technique it is possible to solve for the entry angle and consequently for the maximum stress angle and the corresponding sinkage of each mass element.

4.4 Bulldozing Effect

The bulldozing effect is created when a volume of the soil in the contact patch is displaced to the sidewall of the tire. As such, a lateral force is created on the sidewall of the tire. A graphical representation of this phenomenon can be observed in **Error! Reference source not found.**.

Few tire models account for the bulldozing component of the lateral force. Those that incorporate it, applied it at the single mass that represented the contact patch. In the current study, due to the discretization of the tire, the bulldozing effect can be applied directly on the sidewall elements, thus increasing the realism of the model.

Thus, a bulldozing force will be applied at each mass, which is also a more realistic representation. The formulation used to determine the bulldozing effect is based on the principle of passive ground resistance developed by Terzaghi, which is presented in [22]. This formulation has different dimensionless soil resistance coefficients that according to Wong [2] are dependent on the soil angle of friction φ. On the other hand, q is the surcharge load from the accumulated soil, which is calculated by assuming that the soil displaced in the lateral direction on each side of the wheel is the same as the volume of soil accumulated for the surcharge load.

$$F_{ybd,i} = \left(\gamma_s z_i^2 N_\gamma + c z_i N_c + q_i z_i N_q\right) \cos \delta_f \quad (20)$$

$$q_i = \frac{\gamma_s V_{soil}}{m z(\theta)} \quad (21)$$

$$m \approx \tan\left(\frac{\pi}{4} + \frac{\phi}{2}\right) \quad (22)$$

4.5 Multi-pass Effect

The multi-pass is a really important effect for soft soil interaction. The impact of a tire on soil is dependent on a variety of factors. One such factor is the type of pass. A towed wheel will not alter the properties of the terrain in the same manner as a driven wheel, which induces larger changes [24-25].

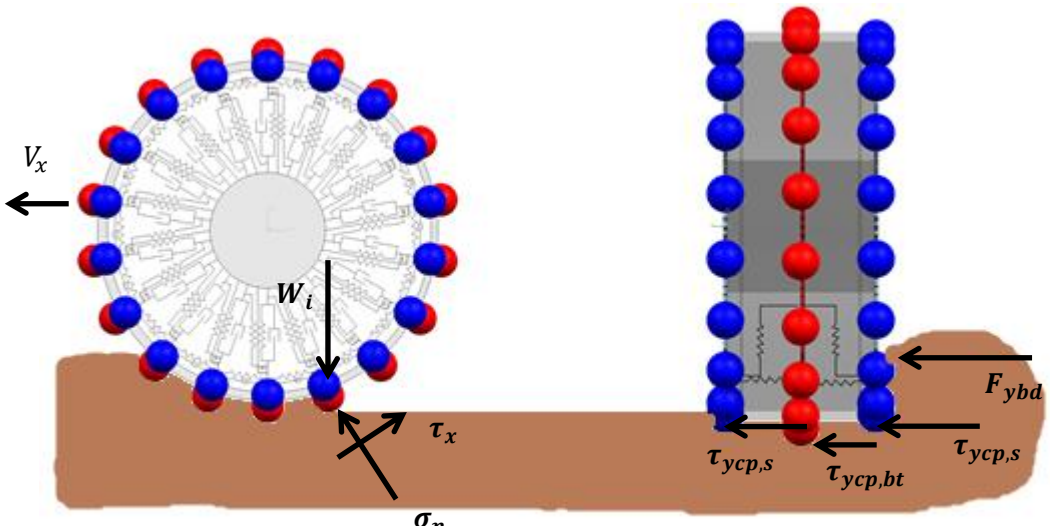

Fig. 6: *Graphical representation of the bulldozing effect and shear stresses*

The number of passes also has an influence on the terrain properties. Moreover, the slip ratio also affects the soil properties for multi-pass.

The approach used in this study to quantify the multi-pass effect will rely on the work of Holm [26] and Senatore [27], and its main idea is to estimate new parameters for the soil based on the pass type and slip.

4.6 Forces and Moments

4.6.1 Longitudinal Force/Drawbar Pull

The drawbar pull is one of the most important performance metrics in off-road driving, and it gives the measure of the capability of the vehicle to perform work, such as pulling a trailer or a plow. The drawbar pull is computed in the same way for all the masses in the three planes using Eq. (23). The total drawbar pull will be computed using Eq. (24).

$$F_{x,i} = DP_i = \tau_{x,i}\cos\theta_i - \sigma_{n,i}\sin\theta_i \tag{23}$$

$$F_x = \sum_{i=1}^{3N_m} F_{x,i} \tag{24}$$

4.6.2 Lateral Force

The calculation of the lateral force is also very important, especially for steering maneuvers. Note that the lateral force is made up of two components, which are produced by the (i) lateral shear stress and by (ii) the bulldozing effect. For the sidewall elements the lateral force is calculated using Eq. (26), while for the belt and tread the lateral force is computed using Eq. (25). The total lateral force is given by Eq. (27).

$$F_{y,belt,i} = \tau_{ycp,i} \tag{25}$$

$$F_{y,sidewall,i} = F_{ybd,i} + \tau_{ycp,i} \tag{26}$$

$$F_y = \sum_{i=1}^{3N_m} F_{y,sidewall,i} + F_{y,belt,i} \tag{27}$$

4.6.3 Driving Torque

The driving torque is calculated using Eq.(28), where W_i is the wheel load at each mass.

$$T = \sum_{i=1}^{3N_m} R_{l,i}\left[\tau_{x,i} - W_i\cos\theta_i\right] \tag{28}$$

4.6.4 Overturning Moment

The overturning moment at the axle is a great indicator of performance in handling situations and it is calculated using Eq. (29).

$$M_x = \sum_{i=1}^{3N_m} -W_i y_i - F_{y,i}R_{l,i}\cos\theta_i \tag{29}$$

4.6.5 Self-Aligning Torque

The calculation of the self-aligning torque at the axle follows the same approach of the overturning moment, and is done using Eq. (30).

$$M_z = \sum_{i=1}^{3N_m} R_{l,i}\left[F_{y,i}\sin\theta_i + \tau_{x,i}y_i\right] \tag{30}$$

5 Model Validation

In order to insure the accuracy of the proposed tire model and provide the semi-analytical model with input parameters, it is imperative that well-controlled experimental testing is performed.

The proposed design of experiments for the validation testing is thoroughly explained in this paper. The testing will be primarily performed on a single-wheel testing platform, the Terramechanics rig in the Advanced Vehi-

cle Dynamics Lab (AVDL) at Virginia Tech. More detailed information about the design and instrumentation on the rig are found in [28]. The Terramechanics rig was designed to simulate various road surfaces, to apply normal load, and to measure the forces and moments caused by the tire-soil interaction. Testing can also be performed at different toe and camber angles, as well as at different soil compaction, moisture, and depth levels to replicate real-world conditions.

A statistically relevant design of experiments was drafted to obtain optimal data. The Terramechanics rig carriage, shown in Fig. 7, allows a tire to be tested while the data acquisition program on the central computer allows the user to vary certain parameters during the run. A key parameter that will be varied in a wide range of values is the longitudinal slip of the tire, which is controlled by the two separate motors, of the rig carriage and of the actual wheel, respectively.

Fig. 7: *Terramechanics rig carriage equipped with a pneumatic tire*

Before testing on the sandy loam selected for this study, a series of tests on a rigid surface have been performed to insure the correct calibration and the accuracy of the sensors used on the rig. The hardware on the Terramechanics rig is inspected and, if needed, calibrated after every run, in order to avoid any drift in the data collection.

Figure Fig**. 8** illustrates the drawbar pull results obtained recently while testing a Goodyear P255/55R18 104 H generic winter tire at a 5.18 kN normal load on the rigid platform in the rig.

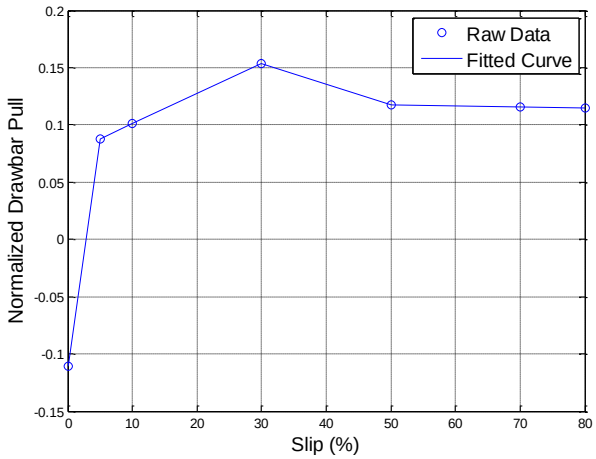

Fig. 8: *Normalized drawbar pull plotted against slip*

By inspecting Fig. 8, one can notice that the normalized drawbar pull-versus-slip curve follows the expected behavior of a tire on a rigid surface. While the tests on sandy loam are still to be conducted, this preliminary work is illustrative of the type of experimental results to be obtained, as well as of the large range of slip ratios that can be employed.

5.1 Test Parameter Selection

The design of experiment is mainly focused on varying the longitudinal slip and the normal load. Because we are interested in observing how these parameters affect the tire performance, different levels per parameter will be tested. As recommended by the industry quad members of the project, the tire behavior at longitudinal slips larger than 65% will be investigated since it is at such high slip ratios that the tire performance on soft soil is less understood. The tires will be tested at two normal loads (100% and 150% of the nominal load) and at two slip angles.

5.2 Tires Selection

The experimental study is scheduled to be performed on two different types of tires. One of the tires is the Goodyear Wrangler SilentAmor P265/70R18 (81.3 cm diameter) tire. This is a large, all-terrain, light-truck tire that is highly rated for its performance on dry, wet-, and off-road applications which rank 9, 9, and 8 out of 10, respectively, on the Good-

year website [29]. The second is a Goodyear Rawhide III which is a smaller (63.5 cm diameter), all-terrain vehicle (ATV) tire. This tire has a rugged, deep-bite tread pattern made for soft terrain applications, super rigid sidewall, and is the common OEM tire choice for many Gators, ARGO, and Honda ATVs.

5.3 Soil Parameters

The process of reconditioning the soil after every test run will certainly be strenuous for the experiment, as it will mostly be executed by hand, so the minimal amount of variance in soil parameters is best. The soil of choice in this study is sandy loam, which is a good compromise between non-cohesive sand and very cohesive clay. An amount of 7.26 metric tons of sandy loam donated to the project by Egypt Farms provides sufficient soil for testing the tires of interest without the results being affected by the boundary conditions (rigid surface under the soil and the rig side walls).

Two different soil moisture content levels between 0% and 30% will be used.

Another soil parameter of high interest is the soil compaction. A Rimik cone penetrometer CP 40 II is employed to test the compaction resistance of the soil. Using generic sandy loam data found in [5], a simplified form of Bekker's equation was used to estimate a normal range of compaction resistance for such a soil. Within this range, the compaction resistance between 333 N and 445 N has been chosen for testing.

5.4 Other Parameters of Interest

To help validate tire forces during steering maneuvers, tests must be performed for non-zero camber and toe angles. The rig was designed to accommodate a camber angle between 0 and 8 degrees and a toe angle from -45 to 45 degrees. The levels of camber selected for this study are 0 and 4 degrees. For the toe, the levels are -15 and +15 degrees.

5.5 Initial Design of Experiment

All the parameters previously mentioned have been compiled into the following design of experiments testing matrix in : Initial *design of experiment test matrix*. The design of experiments will be processed using statistical software to insure statistically relevant and repeatable results. The software will provide the recommended number of runs per test [30]. In deciding the final number of runs conclusions of past studies conducted at WES will also be considered [2,16]

Table 1: *Initial design of experiment test matrix*

Parameter	No. of Levels	Range
Slip Percentage	8	20 - 100%
Normal load	2	100% and 150% nominal load
Inflation Pressure	2	75% and 100% max pressure
Moisture Content	2	0 and 30%
Compaction Resistance	2	333-445 N
Toe Angle	2	0 deg and 30 deg
Camber Angle	2	0 deg and 4 deg

6 Conclusions

This paper presents a proposed semi-analytical soft soil tire model and its experimental validation methodology. The model is intended for traction, ride, handling, and durability applications. The work on the project is ongoing and simulation results as well as validation tests will be presented in future publications.

7 Acknowledgements

The work has been supported in part by the Automotive Research Center (ARC), a U.S. Army RDECOM Center of Excellence for Modeling and Simulation of Ground Vehicles led by the University of Michigan, and in part by NSF through award no. CMMI-0700278. The authors would also like to thank our ARC quad members for their continued support and guidance throughout the project, and to Mr. Anake Umsrithong for fruitful communications on this topic.

Nomenclature

b	Tire width
β	Initial radius approximation dimensionless variable
c	Soil cohesion
c_0	Experimental constant used to determine θ_m
c_i	Multipass experimental parameter
c_{sd}	Multipass experimental parameter
c_m	Experimental constant used to determine θ_m
δ	Tire deformation
k_x	Longitudinal shear deformation modulus
k_y	Lateral shear deformation modulus
k_{xi}	Multipass experimental parameter
k_{sd}	Multipass experimental parameter
k_0	Static modulus of soil deformation
k_1	Sidewall radial spring stiffness (in-plane)
k_2	Wheel-sidewall radial spring stiffness (in-plane)
k_3	Inter-element radial spring stiffness (in-plane)
k_4	Tangential inter-element spring stiffness (in-plane)
k_5	Lateral inter-element spring stiffness (out-of-plane)
k_6	Radial inter-element spring stiffness (out-of-plane)
c_1	Sidewall radial damping (in-plane)
c_2	Sidewall circumferential damping (in-plane)
c_3	Lateral inter-element damping (out-of-plane)
c_4	Wheel-sidewall radial damping (in-plane)
R_l	Loaded radius
R_u	Un-deformed radius
s_d	Longitudinal slip
V_x	Vehicle longitudinal velocity
z_0	Maximum sinkage
n	Pressure-sinkage index
m	Penetration velocity exponent
m_{bead}	Bead mass
$m_{i,bt}$	Belt plus tread element mass
m_{thread}	Tread mass
m_{belt}	Belt mass
$m_{sidewall}$	Total sidewall mass
$m_{i,s}$	Sidewall element mass
m_{wheel}	Wheel mass
N_m	Number of masses
σ_n	Normal stress
τ_x	Longitudinal shear stress
τ_y	Lateral shear stress
j_x	Longitudinal shear displacement
j_y	Lateral shear displacement
p	Radial pressure
p_t	Tire internal pressure
ϕ	Soil angle of internal friction
γ	Soil density
γ_s	Unit weight of soil
γ_{si}	Multipass experimental parameter
γ_{sd}	Multipass experimental parameter

N_γ	Soil specific weight coefficient
N_c	Soil cohesion coefficient
N_q	Soil surcharge load coefficient
q	Surcharge load from accumulated bulldozed soil
z	Sinkage
ζ	Initial radius approximation dimensionless variable
$\dot{z}$	Vertical penetration velocity
z_0	Maximum sinkage
δ_f	Angle of friction between soil and tire
θ	Central angle describing mass position
θ_a	Angle of transition
θ_b	Trailing Edge Angle
θ_e	Entry angle
θ_f	Leading edge angle
θ_m	Angle of maximum normal stress
θ_r	Exit angle
α_c	Slip angle
y	Lateral distance from tire center
ψ	Toe Angle

References

[1] Rauh, J. and Mössner-Beigel, M., 2008, "*Tyre simulation challenges,"* Vehicle System Dynamics, Vol. 46, Supplement, pp. 49-62.

[2] Wong, **J. Y.,** 2008, "*Theory of Ground Vehicles,"* 4th Edition.

[3] Wismur, R. D. and Luth, H.J., 1973, "*Off-road traction prediction for wheeled vehicles,"* Journal of Terramechanics, Vol. 10, pp. 49-61.

[4] Wismur, R. D. and Luth, H.J., 1974, "*Off-road traction prediction for wheeled vehicles,"* Transactions of the ASAE 7, pp. 8-14.

[5] Brixius, W., 1987, "*Traction Prediction Equations for Bias-ply Tires,"* Transactions of the ASAE (871622), ASAE, St. Joseph, MI.

[6] Upadhyaya, S., K. and Wulfsohn, D., 1993, "*Traction Prediction Using Soil Parameters Obtained with An Instrumented Analog Device,"* Journal of Terramechanics, Vol. 30 (2), pp. 85 – 100.

[7] Gipser, M., 2005, *"FTire: a physically based application-oriented tyre model for use with detailed MBS and finite-element suspension models,"* Vehicle System Dynamics 43(1), pp. 76-91.

[8] Gallrein, A., Backer, M., 2007, "*CDTire: a tire model for comfort and durability applications*," Vehicle System Dynamics 45, pp. 69-77.

[9] Fandre, A., Oertel, Ch., 2001, *"Tyre Models in Vehicle System Dynamics: RMOD-K and SIMPACK,"* Anhalt University of Applied Sciences.

[10] Chan, B. J., 2008, "*Development of an Off-road Capable Tire Model for Vehicle Dynamics Simulation*," Ph.D. Dissertation, Virginia Polytechnic Institute and State University, Blacksburg, VA.

[11] Lee, J. H., Liu, Q., Zhang, T., 2005, "*Predictive Semi-Analytical Model for Tire-Snow Interaction*," SAE.

[12] El-Gawwad, K. A., Crolla, D.A., Soliman, A.M.A., and El-Sayed, F.M., 1999, "*Off-Road Tyre Modelling I: The Multi-Spoke Tyre Model Modifed to Include The Effect of Straight Lugs,"* Journal of Terramechanics, Vol. 36, pp. 3-24.

[13] El-Gawwad, K. A., Crolla, D.A., Soliman, A.M.A., El-Sayed, F.M., 1999, "*Off-Road Tyre Modelling II: Effect of Camber on Tyre Performance,"* Journal of Terramechanics, Vol. 36, pp. 25-38.

[14] Harnisch, C., Lach, B., Jakobs, R., Troulis, M. and Nehls, O., 2005, *"A new tyre soil interaction model for vehicle simulation on deformable ground,"* Inter-

national Journal of Vehicle Mechanics and Mobility, Vol. 43.

[15] Shoop, S., 2001, "*Finite Element Modeling of Tire-Terrain Interaction*," PhD Dissertation, University of Michigan, Ann Arbor.

[16] Murphy, N. R., Green, **A. J.,** 1969, "*Effects of Test Techniques on Wheel Performance,"* Journal of Terramechanics, Vol. 6, pp. 37-52.

[17] Kawase, Y., Nakashima, H., and Oida, A., 2006, "*An Indoor Traction Measurement System for Agricultural tires,"* Journal of Terramechanics, Vol. 43, pp. 317-327.

[18] Yahya, A., Zohadie, M., Ahmad, D., Elwaleed, A., and Kheiralla, A., 2007, "*UPM Indoor Tyre Traction Testing Facility'"* Journal of Terramechanics, Vol. 44, pp. 293-301.

[19] Schwanghart, H., 1991, "*Measurement of Contact Area, Contact Pressure and Compaction Under Tires in Soft Soil,"* Journal of Terramechanics Vol. 28, Issue 4, pp. 309-318.

[20] Freitag, D. R. et al., 1970, *"Performance Evaluation of Wheels for Lunar Roving Vehicles,"* U.S. Army Engineer Waterways Experiment Station, March.

[21] Woodward, **A.,** 2011, "*Experimental Analysis of the Effects of the Variation of Drawbar Pull Test Parameters for Exploration Vehicles on GRC-1 Lunar Soil Simulant*,"M.S. Thesis, Virginia Polytechnic Institute and State University, Blacksburg, VA.

[22] Schwanghart, H., 1968, "*Lateral Forces on Steered Tyres in Loose Soil,"* Journal of Terramechanics, Vol. 5, Issue 1, pp.9-29.

[23] Grahn, M., 1999, "*Prediction of Sinkage and Rolling Resistance for Off-The-Road Vehicles Considering Penetration Velocity,"* Journal of Terramechanics, Vol. 28, Issue 4, pp. 339-347.

[24] Wong, J., Y. and Reece, A., R., 1967, *"Prediction of Rigid Wheel Performance Based on the Analysis of Soil Wheel Stresses. Part I: Performance of Driven Rigid Wheels,"* Journal of Terramechanics, Vol. 4, Issue 1, pp. 81 – 98.

[25] Wong, J., Y. and Reece, A., R., 1967, *"Prediction of Rigid Wheel Performance Based on the Analysis of Soil Wheel Stresses. Part II: Performance of Towed Rigid Wheels,"* Journal of Terramechanics, Vol. 4, Issue 2, pp. 7 – 25.

[26] Holm, I. C., 1969, *"Multi-Pass Behaviour of Pneumatic Tires,"* Journal of Terramechanics, Vol. 6, Issue 3, pp. 47-71.

[27] Senatore, C., 2010, *"Prediction of Mobility, Handling, and Tractive Efficiency of Wheeled Off-Road Vehicles,"* Ph.D. Dissertation, Virginia Polytechnic Institute and State University, Blacksburg, VA.

[28] Sandu, C., Taylor, B., Biggans, J., and Ahmadian M., 2008, "*Building Infrastructure for Indoor Terramechanics Studies: The Development of a Terramechanics Rig at Virginia Tech*," Paper no. 30, 9 pg, Proc. of 16th ISTVS Int. Conf., Nov. 25-28, Turin, Italy.

[29] The Goodyear Tire & Rubber Company., 2011, Retrieved June 5th, 2011, from http://www.goodyear.com/

[30] Laboratory for Interdisciplinary Statistical Analysis at VT., 2011, JMP